Analysis and Optimization of Radial Force of Permanent Magnet Synchronous Hub Motors

Zhou Shi[1], Xiaodong Sun[1], Gang Lei[2], Zebin Yang[3], Youguang Guo[2], and Jianguo Zhu[2]

[1]Automotive Engineering Research Institute, Jiangsu University, Zhenjiang 212013, China
[2]School of Electrical and Data Engineering, University of Technology Sydney, NSW 2007, Australia
[3]School of Electrical and Information Engineering, Jiangsu University, Zhenjiang 212013, China

Permanent magnet synchronous hub motors (PMSHMs) have been investigated for electric vehicles. However, there are some challenges, such as effective cooling and radial force. As PMSHMs are installed on the wheels, the radial force will directly affect the ride comfort of the vehicle. This paper presents the analysis and optimization of radial force for PMSHMs. The radial force densities of symmetry and asymmetry PMSHMs are analyzed first. It is found that symmetry PMSHMs have balanced force, while asymmetry PMSHMs normally have big unbalanced radial force and vibration. To reduce the radial force of asymmetry PMSHMs, an improved sequential Taguchi optimization method (ISTOM) with mixed orthogonal array is presented for an asymmetry PMSHM in this study. It can be found that the proposed method is efficient and can significantly reduce the radial force of the hub motor.

***Index Terms*—Permanent magnet synchronous hub motors; radial force, sequential optimization method; Taguchi method.**

I. Introduction

The development of electric vehicles (EVs) has become the mainstream direction of the automobile industry under the pressure of energy and environment. EVs with hub motors subvert the transmission system of the traditional vehicle, which is very helpful to the layout of the vehicle. Thus, hub motor driven EVs have become one of the research hotspots of EVs [1-5]. Permanent magnet synchronous hub motors (PMSHM) have been widely used in hub motors because of the high torque density and high stability.

In most PMSHMs, the fractional-slot concentrated is adopted to reduce the end winding length and to avoid excessive slot number. However, fractional-slot concentrated windings contain a large number of tooth harmonics with lower harmonic frequency which will cause serious vibration and noise. In addition, the radial vibration of the motor will have a greater impact on vehicle ride comfort as the motor changes from the top mass to the bottom mass. Especially for the motor with asymmetry design, as the radial force cannot have balanced each other, it has a large unbalanced radial force [6-8]. Therefore optimize the structure to reduce the unbalanced radial force without sacrificing other electromagnetic performance.

In this paper, a 50-poles PMSHM with different slot number will be analyzed. First, the air gap magnetic field of the PMSHM is analyzed by analytic method. The analytical equation of air gap magnetic field is verified by finite element analysis (FEA). Second, the electromagnetic force of the PMSHM with asymmetry and symmetry structures are analyzed by analytical equation of the air gap magnetic field. The results show that the radial force of asymmetry motor is significantly larger than that of symmetry motor. Then an improved sequential Taguchi optimization method (ISTOM) will be presented to optimize the structure parameters of the asymmetry PMSHM. Finally, the effectiveness of the proposed optimization method will be validated by comparing with the conventional optimization method.

II. Electromagnetic Force Analysis of PMSHM

The radial force (f_{rad}) density and tangential force (f_{tan}) density in a motor can be expressed as

$$f_{\text{rad}} = \frac{1}{2\mu_0}(B_r^{\,2} - B_t^{\,2}) \tag{1}$$

$$f_{\text{tan}} = \frac{1}{\mu_0}(B_r B_t) \tag{2}$$

where μ_0 is the air permeability, B_{r} the radial air gap flux density, and B_t the tangential air gap flux density. The conversion between polar components to Cartesian components of the Maxwell stress tensor is given by the following expressions.

$$\begin{cases} f_{\text{x}} = f_{\text{rad}}\cos\theta - f_{\text{tan}}\sin\theta \\ f_{\text{y}} = f_{\text{rad}}\sin\theta + f_{\text{tan}}\cos\theta \\ f_{\text{rad}} = f_{\text{x}}\cos\theta + f_{\text{y}}\sin\theta \\ f_{\text{tan}} = -f\sin\theta + f_{\text{y}}\cos\theta \end{cases} \tag{3}$$

where θ is the rotor angle in mechanical degrees. The total force acting on the rotor (unbalanced radial force) in x and y axes is calculated as

$$\begin{aligned} F_{\text{x}} &= l\cdot\int_0^{2\pi} r\cdot f_{\text{x}}(\theta)d\theta \\ F_{\text{y}} &= l\cdot\int_0^{2\pi} r\cdot f_{\text{y}}(\theta)d\theta \\ F_{\text{r}} &= \sqrt{F_{\text{x}}^{\,2} + F_{\text{y}}^{\,2}} \end{aligned} \tag{4}$$

where F_x and F_y are the total force acting on the rotor in x axis and y axis, respectively, F_r is the total unbalanced radial force.

III. Finite Element and Experimental Analyses

Fig. 1 shows the radial and tangential air-gap flux density distributions in two PMSHMs with the same poles (50 poles) and different slots (48 and 51 slots). Fractional slot short-distance winding structure is used for both PMSHMs with different slots. As shown, the air-gap flux density of both structures has a large number of high order harmonics which will cause the high order harmonics in the radial force density.

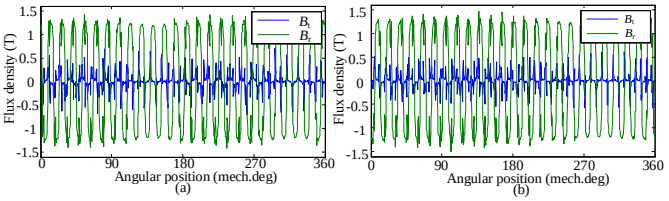

Fig. 1. Radial and tangential air-gap field distributions in PMSHMs, (a) 48slots-50poles, and (b) 51slots-50poles.

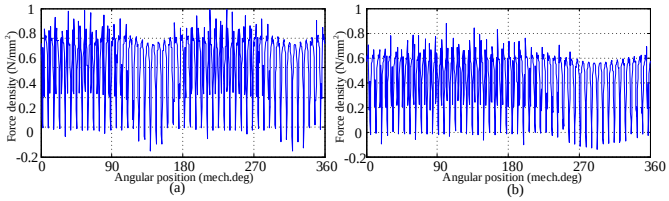

Fig. 2. Open-circuit radial force densities, (a) 48slots-50poles. (b) 51slots-50poles.

Fig. 2 illustrates the radial force of the two motors. As shown, the radial force density of 48-slots motor (symmetry structure) has two periods in the whole mechanical angle, which is different from that of 51-slots PMSHM (asymmetry structure). It means that the radial forces acting on the symmetry structure are balanced on the whole circumference. For the asymmetry structure, the unbalanced radial force is often very large as the radial force cannot be balanced.

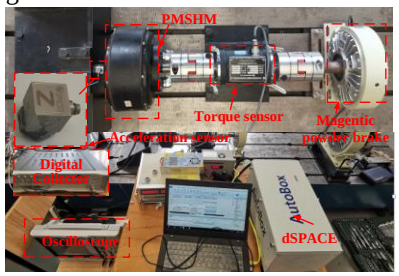

Fig. 3. PMSHM vibration measurement platform.

Fig. 3 shows the vibration measurement platform for two PMSHMs. The PC acquires vibration data from the accelerometers and the oscilloscope monitors the phase currents. The acceleration peaks of two PMSHMs at fixed axes under are tested, respectively. The maximum acceleration of 48slots-50poles PMSHM is 0.56 m/s^2, while the maximum acceleration of 51slots-50poles PMSHM could reach 4.32 m/s^2. The experiment result proves that the vibration of asymmetry motor is greater than that of symmetry motor. However, PMSHMs with asymmetrical structure often have lower torque ripple than symmetry motors and are widely used in hub motors. Thus, it is necessary to decrease the radial force of asymmetry PMSHMs by appropriate optimization methods. The analysis and experiment result have proved that the vibration of asymmetry motor is greater than that of symmetry motor.

IV. Motor Radial Force Optimization Based on Taguchi Method

Taguchi method is a statistical approach to improve the quality of components/products based on design of experiments (DoE) [9-10]. It can be used to minimize the radial force of the asymmetry PMSHM. Fig. 4 illustrates a parameterized model of the asymmetry PMSHM (51 slots/50 poles). Through design experience, seven parameters are selected to reduce the radial force of this motor, and they are: stator outer radius (R_{so}), air gap (δ), slot opening depth (h_{s0}), stator tooth width (l_{tw}), height of stator tooth (h_t), slot width (B_{s0}), and PM arc coefficient (α_{PM}).

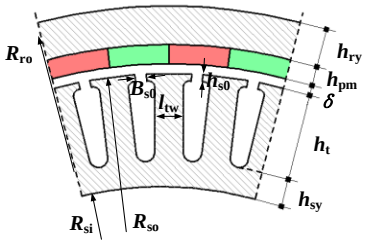

Fig. 4. A parameterized model of the studied asymmetry PMSHM motor

TABLE I
INITIAL VALUES AND LEVELS FOR DESIGN FACTORS

Parameters	Intial	Level 1	Level 2	Level 3
A: R_{so}	96	95.5	96.0	96.5
B: δ	1.5	1.3	1.5	1.7
C: h_{s0}	1.0	0.8	1.0	1.2
D: l_{tw}	5.6	5.4	5.6	5.8
E: h_t	16.0	15.0	16.0	17.0
F: B_{s0}	1.80	1.6	1.8	2.0
G: α_{PM}	0.85	0.8	0.85	0.9

TABLE II
AN ORTHOGONAL ARRAY L18(3^7)

Number	Design parameters						
	A	B	C	D	E	F	G
1	1	1	1	1	1	1	1
2	1	2	2	2	2	2	2
3	1	3	3	3	3	3	3
…	…	…	…	…	…	…	…
17	3	2	1	3	1	2	3
18	3	3	2	1	2	3	1

Table I lists the levels for the seven design parameters. Table II lists an orthogonal array with 18 experiments (L$_{18}$(3^7)). To determine the best values of design factors which could reduce the radial force an objective function is defined as follows.

$$Y(i) = \int_0^{2\pi} F_{r\varphi} d\varphi / 2\pi \tag{5}$$

where Y is the average radial force of the whole cycle, $F_{r\psi}$ is the total force, ψ is the rotor position angle. The subscript i (1, 2, ..., 18) is the experiment number. To ensure that the optimization does not sacrifice other performance significantly, the following requirements need to be met as show in (6):

$$\begin{aligned} \text{s.t.} \quad & \frac{1}{n}\sum_{i=1}^{n} T_{\text{ave-}k\text{-}i} \geq 0.98 \cdot T_{\text{ave-initial}} \\ & \frac{1}{n}\sum_{i=1}^{n} T_{\text{rip-}k\text{-}j}\% \leq 0.98 \cdot T_{\text{rip-initial}}\% \\ & \frac{1}{n}\sum_{i=1}^{n} \eta_{\text{rated-}k\text{-}i} \geq 0.99 \cdot \eta_{\text{rated-initial}} \end{aligned} \tag{6}$$

where T_{ave} and T_{rip}% are the average torque and torque ripple, respectively, η_{rated} is efficiency of the rated working point, and the subscript initial stands for the initial design. The subscript k (1, 2, ..., 7) is the control factor number. The best combination of the levels and values of all design parameters can be found by using the Taguchi analysis method. Based on the obtained Taguchi design, the average radial force is 154 N, which is just slightly smaller than that of the initial design (170 N). Detailed results are listed in the next section. The improvement is not significant. There are two main reasons for this small improvement (or two shortcomings for the Taguchi method). First, the levels of Taguchi method are quite close (small step sizes) and are mainly designed by experience Second, as this motor has 7 factors, it is a high dimensional design problem. If the same level number is assigned for all parameters, it is harder to find optimal values for those significant factors compared with those non-significant factors. To overcome the first issue, a sequential Taguchi optimization method was presented [9]. However, it is efficient for low-dimensional (dimension no more than 5), instead of high-dimensional problem. In addition, conventional Taguchi design is only suitable for small range optimization. If large range is applied, the factor levels should be increased to ensure the accuracy of optimization result, which will increase the FEMs. Thus, to overcome the second shortcoming, an improved sequential Taguchi optimization method (ISTOM) based on mixed orthogonal table is proposed in this study.

V. Improved Sequential Taguchi Optimization Method

The flowchart of the proposed ISTOM is shown in Fig. 5. It includes four main steps.

Step 1: Define the objective function, optimization constraints, optimization parameters and their ranges (or the initial design space) for the PMSHM.

Step 2: Calculate the sensitivity of each design factor by using the Pearson correlation analysis method.

$$\rho_{X,Y}=\frac{N\sum XY-\sum X\sum Y}{\sqrt{N\sum X^2-(\sum X)^2}\sqrt{N\sum Y^2-(\sum Y)^2}} \tag{7}$$

where Y is the optimization objective (average radial force), X is the design parameters, and N is sample size. According to the results of correlation analysis, more levels can be assigned to the factors with high correlations, while less levels can be assigned to the factors with low correlations.

Step 3: Develop a mixed orthogonal array and implement the analysis to find the best combination of levels for all design parameters, then a Taguchi design is obtained. Compute the average radial force of the motor for the obtained Taguchi design and compare it with the force of the initial design. If the relative error between them is less than ε (a positive value like 5%), finish the optimization process and output the obtained optimal design. Otherwise, go to the next step and re-implement the Taguchi parameter design process.

Step 4: Reduce the range of the design parameters by using the obtained Taguchi design and space reduction method and update the levels of each design factor and the corresponding orthogonal table. For example, assume the initial design space of a design factor is [a, b]. If this factor is a significant one, four levels will be assigned, otherwise, two levels will be assigned. If the optimal value of this factor is x_0 after Taguchi analysis, then the next four levels or two levels will be

$$\begin{cases}[a,a+d,a+2d,a+3d], & x_0-d\le a\\ [b-3d,b-2d,b-d,b], & x_0+d\ge b\\ [x_0-3d/2,\ x_0-d/2, & \\ \ x_0+d/2,\ x_0+3d/2,] & \text{others}\end{cases}\ \text{(four levels)}$$
$$\begin{cases}[a,a+d/2], x_0=a\\ [b-d/2,b], x_0=b\end{cases}\ \text{(two levels)} \tag{8}$$

where d is the step size between two levels of design factors.

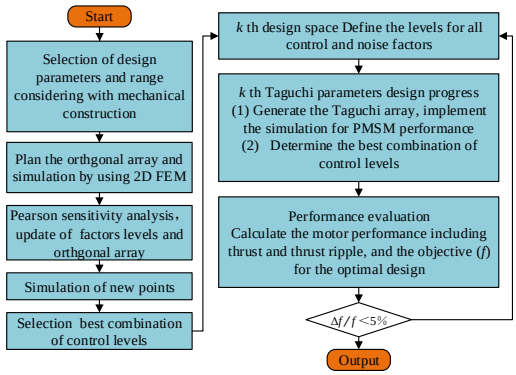

Fig. 5. Flowchart of the improved sequential Taguchi optimization method.

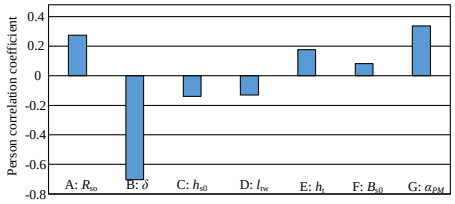

Fig. 6. The Pearson correlation coefficient of seven factors to the radial force.

VI. Optimization Results

Fig. 6 shows the analysis results of Pearson correlation analysis method for this asymmetry PMSHM. Based on the results, 3 parameters are selected as significant factors and others are non-significant factors. Therefore, a mixed orthogonal array $L_{16}(4^3\times2^4)$ as listed in Table III is established.

As shown, this mixed table $L_{16}(4^3\times2^4)$ is different from Table II in which the factors A, B, and G have four levels while factors C, D, E, and F only have two levels. Through this method, the factors with high influence can have more levels, which makes the optimization more effective. Optimization objective Y under the factor A at the fourth level can be computed as (9). The analysis data for each level of factors are shown in Fig. 7. Besides, the factor levels which unsatisfied (6) are marked with (※) in Fig. 7.

$$G_{A3}=\frac{1}{4}\left[Y(13)+Y(14)+Y(15)+Y(16)\right] \tag{9}$$

Table IV lists the final optimal values of the design factors obtained from the proposed ISTOM and the corresponding

motor performance. The average radial forces of the conventional Taguchi design (based on Table II), conventional Taguchi with wider levels and the proposed ISTOM are reduce by 9.41%, 16.4% and 36.0%, respectively, compared with the force of the initial design. Therefore, the proposed ISTOM is efficient. Fig. 8 illustrates the radial force under rated load of the initial design and the optimal design obtained from the proposed ISTOM. As shown, the radial force decreases significantly through ISTOM.

TABLE III
AN ORTHOGONAL ARRAY $L_{16}(4^3\times2^4)$

Number	Control factors						
	A	B	C	D	E	F	G
1	1	1	1	1	1	1	1
2	1	2	1	2	2	2	2
3	1	3	2	3	1	1	3
4	1	4	2	2	2	2	4
5	2	1	2	2	1	2	2
…	…	…	…	…	…	…	…
14	4	2	2	1	1	2	3
15	4	3	1	2	2	1	2
16	4	3	1	2	1	2	1

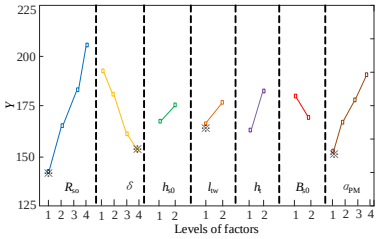

Fig. 7. Average radial force all factors and levels.

TABLE IV
PERFORMANCE COMPARISON

Par.	Initial	Taguchi $L_{16}(3^7)$ OA	Taguchi $L_{16}(3^7)$ OA（wider levels）	ISTOM $L_{16}(4^3\times2^4)$ OA
R_{so}	96	96	95	92.8
δ	1.5	1.5	2	2.15
h_{s0}	1.0	0.8	0.5	0.55
l_{tw}	5.60	5.6	5.8	6.0
h_t	16.0	15.0	15	15.4
B_{s0}	1.80	1.60	1.6	1.62
α_{PM}	0.85	0.85	0.9	0.88
y_i	170	154	142	112

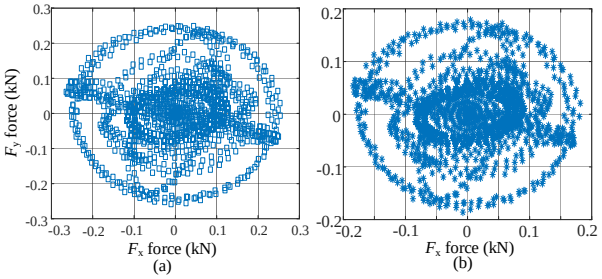

Fig. 8. Radial force under rated load for the (a) initial design, and (b) optimal design given by the ISTOM.

VII. CONCLUSION

In this study, the radial force of two PMSHMs with symmetry and asymmetry topologies were analyzed. It is found that the asymmetry topology of the PMSHM has high radial force which will cause significant vibration in the operation. To reduce the radial force, an ISTOM was presented for this motor as it is a high dimensional optimization design problem and the conventional sequential Taguchi method cannot handle it effectively. The results show that ISTOM is efficient. The average radial force of the motor can be decreased by 36.0% compared with that of the initial design. Besides, the proposed ISTOM improved the optimization efficiency. The proposed method only needs 64 FEMs, while the conventional Taguchi method needs at least 256 FEMs to achieve the same optimization accuracy. The proposed method can be employed to the high-dimensional design optimization of other electrical machines and electromagnetic devices.

ACKNOWLEDGMENT

This work was supported by the National Natural Science Foundation of China under Project 51875261, the Natural Science Foundation of Jiangsu Province of China under Projects BK20180046 and BK20170071, the “Qinglan project” of Jiangsu Province, the Key Project of Natural Science Foundation of Jiangsu Higher Education Institutions under Project 17KJA460005, the Six Categories Talent Peak of Jiangsu Province under Pro-ject 2015-XNYQC-003, and the Postgraduate Research & Practice Innovation Program of Jiangsu Province under Project KYCX17_1815.

REFERENCES

[1] X. Sun, K. Diao, G. Lei, Y. Guo, and J. Zhu. Real-time HIL emulation for a segmented-rotor switched reluctance motor using a new magnetic equivalent circuit. *IEEE Trans. Power Electron.*, DOI: 10.1109/TPEL.2019.2933664, 2019.

[2] Z. Shi, X. Sun, Y. Cai, Z. Yang, G. Lei, Y. Guo, and J. Zhu, “Torque analysis and dynamic performance improvement of a PMSM for EVs by skew angle optimization,” *IEEE Trans. Appl. Supercon.*, vol. 29, no. 2, pp. 1-5, 2019.

[3] X. Sun, C. Hu, G. Lei, Y. Guo, and J. Zhu, “State feedback control for a PM hub motor based on grey wolf optimization algorithm,” *IEEE Trans. Power Electron.*, vol. 35, no. 1, pp. 1136-1146, Jan. 2020.

[4] X. Sun et al, “MPTC for PMSMs of EVs with multi-motor driven system considering optimal energy allocation.” *IEEE Trans. Magnetics*, 2019, 55(7), Art. no.: 8104306.

[5] X. Sun, Z. Shi, G. Lei, Y. Guo, and J. Zhu, "Analysis, design and optimization of a permanent magnet synchronous motor for a campus patrol electric vehicle," *IEEE Trans. Veh. Technol.*, pp. 1-1, 2019. DOI: 10.1109/TVT.2019.2939794

[6] H. Yang and Y. Chen, “Influence of radial force harmonics with low mode number on electromagnetic vibration of PMSM,” *IEEE Trans. Energy Convers.*, vol. 29, no. 1, pp. 38-45, 2014.

[7] Z. Song, Y. Yu, F. Chai, and Y. Tang, “Radial force and vibration calculation for modular permanent magnet synchronous machine with symmetrical and asymmetrical open-circuit faults,” *IEEE Trans. Magn.*, vol. 54, no. 11, pp. 1-5, 2018.

[8] G. Dajaku and D. Gerling, “The influence of permeance effect on the magnetic radial forces of permanent magnet synchronous machines,” *IEEE Trans. Magn.*, vol. 49, no. 6, pp. 2953-2966, 2013.

[9] B. Ma, G. Lei, J. Zhu, et al., “Application-oriented robust design optimization method for batch production of permanent-magnet motors,” *IEEE Trans. Ind. Electron.*, vol. 65, no. 2, pp. 1728-1739,2018.

[10] J. Song, F. Dong, J. Zhao, S. Lu, S. Dou and H. Wang, "Optimal design of permanent magnet linear synchronous motors based on Taguchi method," *IET Electron. Power Appl.*, vol. 11, no. 1, pp. 41-48, 1 2017.